Chapter 11
Nano-emulsions for Drug Delivery and Biomedical Imaging

Nicolas Anton, François Hallouard, Mohamed F. Attia, and Thierry F. Vandamme

Abstract Over the last decade, nano-emulsion has gained a considerable interest in biomedical applications. The reason is simple, and lies in the combination of several advantages of this nano-carrier. Nano-emulsion consists of a dispersion of oil nano-droplets in a water phase, sizing from 20 to 200 nm. First advantage of nano-emulsions is their huge stability; Second is their very simple formulation; Third is their non-toxicity; And fourth is their very important loading capability of lipophilic or oil-soluble molecules in the oily core of the nano-droplets. On the other hand, if the formulation is easy, tailoring the nano-emulsions for a given application, optimizing the processes, functionalizing the droplets surface, and targeting organs or cancerous tumors remains a challenge. This chapter aims to draw an overview of the different aspects of nano-emulsions formulations and applications. A first part regards the different fabrication processes, followed by biomedical applications of nano-emulsions, *in vivo* fate, biodistribution, pharmacokinetics, targeting, applications as nanomedicines and drug delivery systems. Clinical applications of nano-emulsions are also discussed, as well as their applications as contrast agent for the main different imaging modalities, X-ray imaging, fluorescence imaging and magnetic resonance imaging.

N. Anton (✉) • T.F. Vandamme
CNRS UMR 7199, Laboratoire de Conception et Application de Molécules Bioactives, équipe de Pharmacie Biogalénique, University of Strasbourg, 74 route du Rhin, 67401 Illkirch Cedex, France
e-mail: nanton@unistra.fr

F. Hallouard
DC2N Inserm U982, Laboratoire de Pharmacie Galénique Biopharmacie, Faculté de Médicine & Pharmacie, Université de Rouen, Rouen, France

Service de Pharmacie, Centre Hospitalier Asselin Hédelin, Yvetot, France

M.F. Attia
CNRS UMR 7199, Laboratoire de Conception et Application de Molécules Bioactives, équipe de Pharmacie Biogalénique, University of Strasbourg, 74 route du Rhin, 67401 Illkirch Cedex, France

National Research Center, P.O. 12622, Cairo, Egypt

A. Prokop, V. Weissig (eds.), *Intracellular Delivery III*, Fundamental Biomedical Technologies 8, DOI 10.1007/978-3-319-43525-1_11

Keywords Nano-emulsion • Formulation • High-energy method • Low-energy method • Nanomedicines • Targeting • Surface functionalization • Biomedical imaging

Abbreviations

ALA	Aminolaevulinic acid
AK	Actinic keratosis
BF200 ALA	BF200 aminolaevulinic acid
CMC	Critical micelle concentration
CT	Computed tomography
DLS	Dynamic light scattering
DTPA- PE	Diethylenetriaminepentaacetic acid phosphoethanolamine
DTX	Docetaxel
EPR	Enhanced permeation and retention
HLB	Hydrophilic-lipophilic balance
IONPs	Iron oxide nanoparticles
LNP	Lipid nanoparticle
MAL	5-aminolaevulinic acid
MRI	Magnetic resonance imaging
NIR	Near infrared
NIRF	Near infrared fluorescence
NMR	Nuclear magnetic resonance
NPs	Nanoparticle
PAV	Prednisolone acetate valerate
PBS	Phosphate buffer saline
PET	Positron emission tomography
PDI	Polydispersity index
PEG	Polyethylene glycol
PFCs	Perfluorocarbons
PFPE	Perfluoropolyether
QDs	Quantum-dots
RES	Rethiculoendothelial system
SPECT	Single photon emission computed tomography
SPIO	Superparamagnetic iron oxide
TEM	Transmission electron microscopy
TXT	Taxotere®

11.1 Introduction

Conventional emulsions, also called macro-emulsions, are typically sizing around the micrometer or larger. This is advantageous as regards the formulation process since they can be simply generated with conventional mechanical methods, like rotor-stator devices, but disadvantageous as regards their stability. Size range of macro-emulsions originates many physical destabilization processes, mainly gravitational-based phenomena that favor droplet flocculation and ultimately coalescence. On the other hand, the term "nano-emulsions" refers also to emulsions with the same structure than macro-emulsions but with drastic differences in both their stability properties and formulation processes. First, nano-emulsions (also known as miniemulsions, fine-dispersed emulsions, submicron emulsions and so forth) can be formulated from 10 to 20 nm up to 200–300 nm. In general, emulsions are thermodynamically unstable systems because the free energy ΔG_f is greater than zero. The physical destabilization of emulsions is related to the spontaneous trend to reduce interfacial area between the two immiscible phases. The minimization of interfacial area is attained by two mechanisms: *(i)* flocculation generally followed by coalescence, and *(ii)* Ostwald ripening. The global expression $\Delta G_f = \gamma \Delta A - T\Delta S_f$ (with γ the water–oil interfacial tension, ΔA the water–oil interfacial area gained with emulsification, $T\Delta S_f$ the entropy of droplet formation), means that the emulsion instability only comes from ΔA.

In the case of nano-emulsions, the stability comes from two phenomena; their nano-scale size range inhibits the effect of gravitation to the benefit of Brownian motion, and induces the predominance of the steric stabilization between droplets. As a consequence, Ostwald ripening is the only process that destabilizes the droplet giving a typical stability over several months. Actually, this kinetic stability is the main typical characteristic of nano-emulsions, making them prime candidate for numerous applications from nanomedicine, pharmaceutics, to agro-food industries. In nano-emulsion systems, the very small size of droplets will prevent the droplets undergoing reversible processes like flocculation and creaming (or sedimentation), and thus preventing the coalescence. However, the stability of nano-emulsions actually appears as a paradox since ΔA of nano-emulsions is definitively higher than the one of macro-emulsions, thus resulting in higher ΔG_f. On the other hand, the inhibition of the destabilization processes predominates, resulting in very stable nano-emulsions. Stability of nano-emulsions is an experimental fact, and very easily obtained with simple formulation procedures.

As we saw above the main property of nano-emulsions is their stability, but another interesting point due to the Brownian properties of the droplets is their ability to diffuse in all the available volume to give a very homogeneous dispersion of droplets. Therefore after encapsulating a given active principle (*e.g.* drugs, contrast agents) in oil nano-droplets, these hydrophobic or lipophilic molecules are homogeneously dispersed in the aqueous phase. The nano-scale of nano-emulsions droplets is also an advantage for biological and medical applications since they have privileged interactions with living cells, tissues, organs of pathologies, and they are as

well compatible with the parenteral administration. In that way nano-emulsions naturally found many applications in various fields and notably in nanomedicines as lipid nano-carriers.

11.2 Formulation Processes

11.2.1 Generalities

Emulsification consists of dispersing one fluid into another non-miscible one, creating interface through the increasing of ΔA. The properties of the generated emulsion, *i.e.* size distribution and stability, are closely linked not only to the composition, chemical nature of the phases and stabilizing agents, ratio of viscosities of the dispersed and bulk phases, but also on the formulation protocol, temperature and time of processing, shear rate, cooling time, and type of emulsification apparatus. In addition, besides these criteria, the emulsion stability is strongly related to the size distribution of the dispersion after formulation. In the case of nano-emulsion, monodispersity will have a direct impact on the inhibition of Ostwald ripening, since the difference of the pressure between the bigger and smaller droplets will be reduced. The formulation of emulsions is conditioned by the energy supplied by the formulation device. Actually, most of apparatuses currently used for the fabrication of macro-emulsions do not allow decreasing the droplet size below 1 μm because of low emulsification yields due to the dissipation of the mechanical energy in heat. It is for example the case of rotor/stator apparatus like UltraTurrax® and colloidal mills. Only some methods allow the fabrication of nano-emulsions. Table 11.1 gathers the main methods for the formulation of emulsions along with the range of the generated droplet sizes (with limiting $\phi_v^d < 30\,\%$ to avoid droplet recombination during processing).

It follows that the three main possibilities for the formulation of nano-emulsions are: *(i)* high-pressure homogenization, *(ii)* ultrasound based methods (using sonotrode), and *(iii)* low-energy emulsification. In the following sections, these

Table 11.1 Summary of the accessible sizes in function of the emulsification apparatuses

Emulsification method	Typical size
Mechanical stirring	1–15 μm
Colloidal Mills	10–50 μm
* High-pressure homogenization	50 nm–5 μm
Membrane	0.2–100 μm
* Microfluidizer®	10 nm–1 μm
* Ultrasonication	20 nm–1 μm
* Low-energy methods	10–200 nm

* the ones generally compatible with the formulation of nano-emulsions

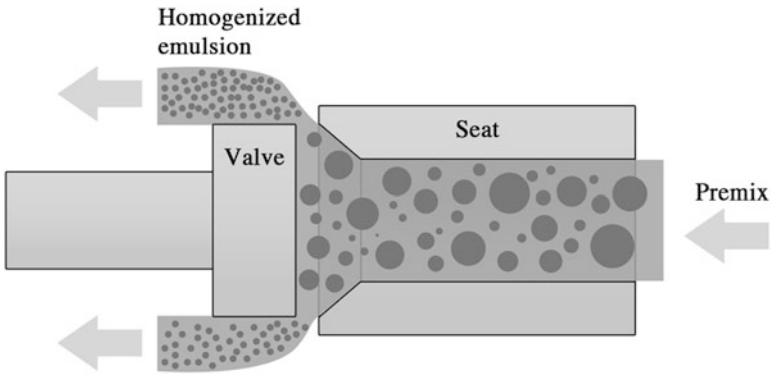

Fig. 11.1 Conceptual representation of high-pressure homogenizer chamber

processes will be presented and the conditions to reach nanometric-sized droplets will be discussed. It is to be noted that in the case of high-energy methods (high pressure or sonication), the formulation of nano-emulsions obligatory follows a preliminary step of pre-emulsification. The initial phase containing all components like emulsifiers, additives, and maintained at controlled temperature, undergoes a stage of dispersion that consist in creating a strong shearing that favors the breaking-up of the drops. Apparatuses indicated for this step are generally turbines type (*e.g.* Rushton type), that provide a high shearing along with an efficient recirculation of the liquid, giving rise to a premix emulsion between 10 and 100 μm. Then, the second step, homogenization step, will decrease the droplet size below 500 nm, narrow the size distribution, eventually improving the stability.

11.2.2 High-Pressure Methods

High-pressure homogenization is a very common industrial process, notably in the formulation of agri-food liquid or semi-liquid products. The premix emulsion is projected under high pressure from 30 to 1'000 bar through a homogenization head of particular geometry (see Fig. 11.1), and undergoes a combination of elongation and shear flows, impacts, and cavitations. The resulting size distributions are reproducible with a mean size ranging from 50 nm to 5 μm.

High-pressure emulsification arises from the competition between the droplets break-up die to deformation enhanced by the high-speed flow, and their recombination due to coalescence enhanced by collisions. The main parameters influencing the size and dispersity of the nano-emulsions are *(i)* the number of passages in the homogenizer, *(ii)* the value of the volume fraction of dispersed phase φ_v^d, *(iii)* the value of the pressure applied, and *(iv)* the concentration C of stabilizing agent like surfactants, proteins, polymers. We can note that the stabilizing agent concentration C is a critical parameter, since, if C is lower than $cmc/10$ (*cmc* is the

critical micelle concentration), the droplet size does not decrease lower than 300 nm. This is due to the predominance of the coalescence against the stabilization of the fragmented droplets. On the other hand, when C is typically higher than $cmc \times 10$, the surfactants molecules are efficient to stabilize the droplets formed after fragmentation, allowing to decrease the size up to 50 nm. Of course, a further increase of C can reach the interface saturation that cannot allow a further decrease of the size. In addition, as easily understandable, this is only in this regime of surfactant concentration that the effect of the applied pressure is effective, actually the size follow a power law (Taisne et al. 1996).

11.2.3 Ultrasounds-Based Methods

This formulation method consists in applying a strong ultrasonic energy in a small volume sample under circulation. This is performed with a specific sonotrode that concentrate the energy in a surrounding volume (see Fig. 11.2). Ultrasonic emulsification is thus only efficient in this small volume around the sonotrode, and thus the fluid circulation in the sample is still necessary for optimizing the process, and as well involves a minimum time before stabilization of the droplet sizes. The frequencies of ultrasound are from 16 kHz to 1 MHz, and generated by a plane surface vibrating on a sinusoidal way with amplitude between 1 and 200 μm. Cavitation bubble alternatively undergo contraction and dilatations, and the micrometric globules of the premix emulsions are broken-up by the successive implosions of the cavitation bubble. The droplet fragmentation of the droplets gradual decreases their average diameter. This is illustrated in Fig. 11.2 (middle) that shows the nanoemulsion mean size describes an exponential decay up to stabilization, for a simple system composed of medium chain triglycerides (oily core), nonionic surfactant (stabilizing agent) and water as continuous phase (Delmas et al. 2011). The figure shows the follow-up of the mean size and polydispersity indexes (PDI). PDI reflects the quality and monodispersity of the dispersion, such that a suspension is considered of good monodispersity (good quality) if the value of PDI is below 0.2–0.15, and of very good monodispersity (very good quality) if the PDI is below 0.1. The exponential profiles reported, for a similar system can be "stretched" if the energy supplied is decreased, as illustrated in Fig. 11.2 (bottom). This result is actually important for understanding the process, as well as its design and optimization. If ultrasound-based technologies are compared with high-pressure homogenizers, the properties of the resulting emulsions are generally similar. However, high-pressure homogenizers are widely used in industrial processes, whereas ultrasonifiers are more adapted for the laboratory scale, research and development stages.

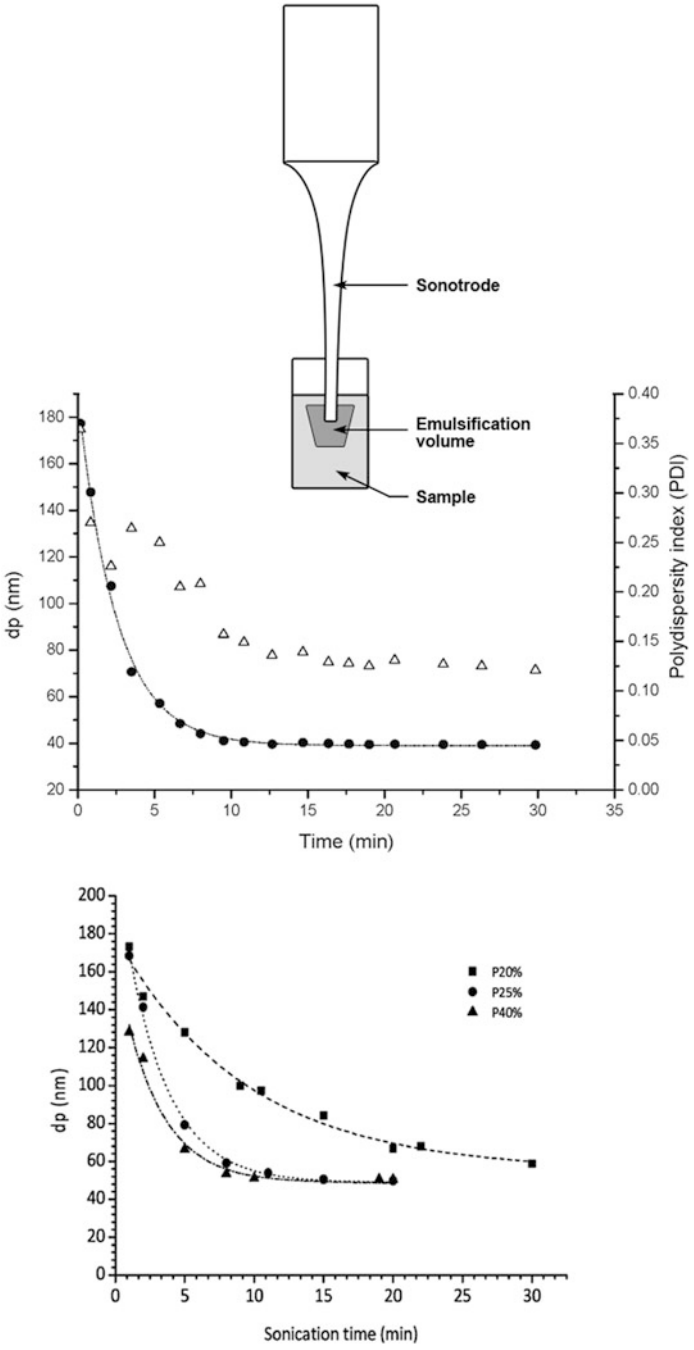

Fig. 11.2 (Reprinted adapted with permission from (Delmas et al. 2011)). *S*chematic of a sonication-based nano-emulsification process. *Top:* evolution of droplet size distribution along the sonication process: particle mean diameter (black disks), and polydispersity index (open triangles). *Bottom:* evolution of droplet size distribution along the sonication process in function of the power of the sonicator

11.2.4 Low-Energy Methods

Low-energy methods allow the formulation of nano-emulsions similar to those described above (with high pressure and sonication methods), but without mechanical energy. In this case, the increase of ΔA is obtained by taking benefit of the intrinsic physicochemical properties of the phases and stabilizing agents.

Low-energy methods are simple, cost-effective formulation processes and are very attractive. However, the low-energy methods are very studied but almost only on the fundamental point of view, and much less used in industrial processes than high-energy ones. This is likely due to several points, like the fact *(1)* that these methods only allow nano-emulsification and not homogenization of premix (*e.g.* not suitable for homogenizing milk), or *(2)* that the physicochemical properties of the dispersion cannot always be finely controlled, or finally *(3)* that they involve a non-negligible amount of surfactants that is not always compatible with all the specifications (impact on the taste in agrifood industries, or induce a toxicity, etc.).

Low-energy methods in general are based on spontaneous emulsification, or self-emulsification. It is to be noted that other low-emulsifications methods are reported, like phase inversion temperature methods of solvent diffusion, but it has recently been shown that their principle is based on the spontaneous emulsification described below. Spontaneous emulsification occurs when two immiscible fluids are brought in contact and gently homogenized. In a few seconds a kinetically stable nano-emulsion is formed. In contrast with high-energy methods, spontaneous emulsification allows a similar gain in ΔA without energy input. Spontaneous emulsification takes benefit of the physicochemical properties of the water, oil, and surfactant for generating the nano-droplets through a spinodal decomposition-like process.

Numerous explanations aimed understanding of this phenomenon, however, it is only recently than a universal and simple mechanism was proposed (Anton and Vandamme 2009), thus including all the spontaneous emulsification processes. Illustrated in Fig. 11.3, the spontaneous emulsification was attributed to the penetration of the water phase in the oily one, resulting in breaking-up the oil phase at the nanometric scale. Let us consider the oil phase homogeneously mixed with surfactant molecules in specific conditions (*e.g.* temperature) that make them lipophilic (Fig. 11.3a). Then, once this surfactant/oil phase is in contact with water (Fig. 11.3b), aqueous phase penetrates the oil one solubilizing the surfactant molecules (Fig. 11.3c). Surfactants stabilize the newly-formed oil nano-droplets generating the nano-emulsions (Fig. 11.3d), generally sizing from 20 nm to 200–300 nm. In addition, spontaneous nano-emulsions give suspension with a very good monodispersity excepted when we reach the limit of the feasibility region, *e.g.* at low surfactant concentrations, where the polydispersity indexes suspensions can increase higher than 0.2–0.3. It follows that spontaneous emulsification is driven by the physicochemical properties of the surfactant and its solubility towards the oily and aqueous phases. On the other hand, when a spontaneous emulsification process is efficient to give nano-emulsions, its own size can be finely controlled by the surfactant concentration, namely the higher is the surfactant concentration, the lower is

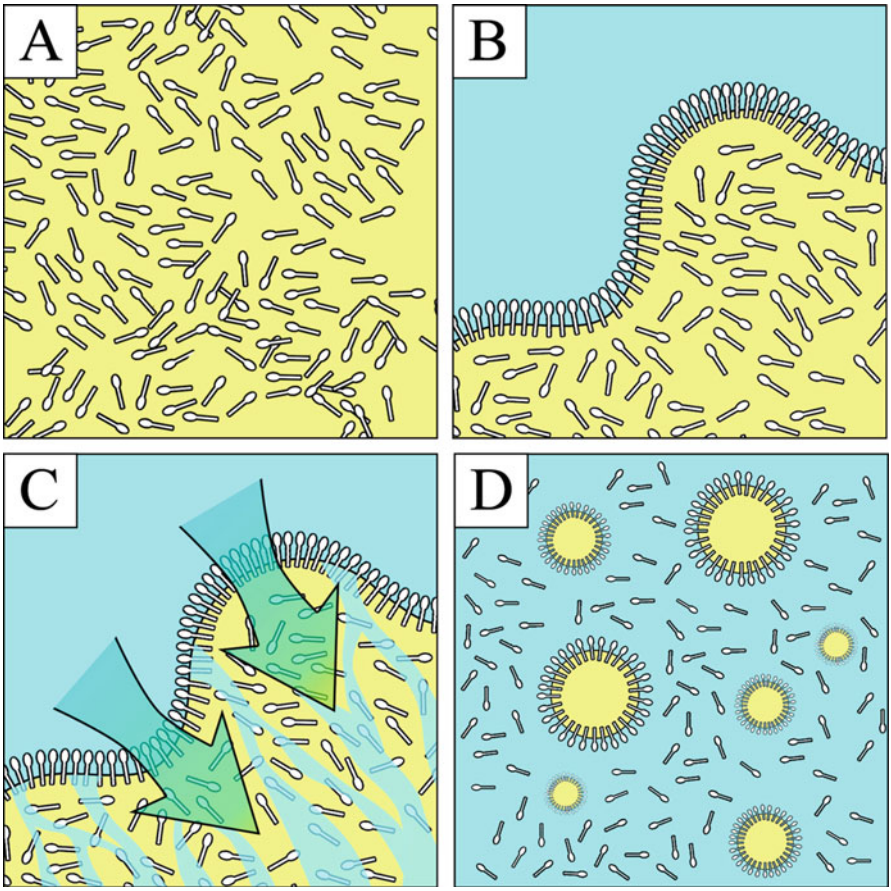

Fig. 11.3 (adapted from (Anton and Vandamme 2009)) Schematic representation of the mechanism driving the spontaneous emulsification

the average nano-emulsion size (Anton and Vandamme 2009). It is noteworthy that not all the surfactant/oil couples are compatible with the spontaneous nano-emulsification, and this is one of the main reasons why sometimes it is necessary to shift to high-energy methods. However, we can define some necessary conditions for the spontaneous emulsification, like the complete solubility of the surfactant to the oily phase. This affinity can be relative and be artificially improved with temperature, for example with nonionic surfactants that become lipophilic at high temperature (above their cloud point in general). Then with a sudden mixing with the aqueous phase at room temperature (*i.e.* colder water) the surfactant affinity for oil is suddenly decrease beneficially to the one of water, enhancing the water penetration. Another important factor that impact on the process is simply the chemical nature of each compound, not only the properties of nonionic surfactant but also the nature of oil, the nature of surfactant, and the additives in the aqueous phase.

11.3 Applications of Nano-emulsions for Drug Delivery and Biomedical Imaging

11.3.1 Nano-emulsions as Nanomedicines

The drugs used for Humans present a main pharmacological activity, but also adverse effects. Thus improving the efficiency of a drug by inhibiting its adverse effects results in increasing its benefit-to-risk ratio. Nanotechnologies, in general, and nano-emulsions being a realistic solution, allow increasing its benefit-to-risk ratio in modifying the becoming of the drug in the organism. This aspect is particularly crucial in antitumor treatments, aiming a very specific targeting on tumor cell without affecting healthy cells. The main strategy consists in associating the drug with a nano-carrier, which will influence the drug biodistribution and elimination. In this case, the drug may follow the *in vivo* fate of the nanocarrier, closely related to its physicochemical properties like size, electrostatic charge, chemical composition, functionalization. Optimizing this operation results in increasing the targeting of the drug towards the tissues in which we want this last one has to be active, increasing the time in contact, while limiting its diffusion to those it could be toxic. This targeting ideally improves the drug efficiency. Actually, the design, the development and the optimization of an efficient vector are not only related to the understanding and expertise in the formulation process of the nanocarriers, sometimes delicate at the nanometric scale, but also on the knowledge of the different physiological, histological, biological and biochemical aspects of the tissues in living organisms. Actually, the biodistribution of the drug will be driven by the interactions and *in vivo* behavior of the nanocarrier in the body. In addition, in function of the administration route, the nano-carrier will be in contact with different tissues and its pathway can be different.

As regards lipid nano-emulsions as drug delivery systems, and considering that the potential drugs are solubilized in oil cores without premature leakage, their targeting properties will be defined by the interactions of the lipid droplets in function of the administration route. Let us now focus on the different administration ways, and evaluate the different potentialities for targeting lipid nano-droplets.

Intravenous administration constitutes the main administration route adopted for research investigations or preclinical studies since blood is the ultimate location desired for a drug before targeting. However, beside physiological compatibilities like sterility, osmolarity and pH, the size of the nanocarrier is a main issue in their design. Once in the bloodstream, the nano-droplets will circulate in the blood pool, migrate to the heart by the vena cava, then in the lung to be back in heart by the pulmonary vena, and in the arterial circulation by the aorta. In this context, the risk of pulmonary emboli that arises above 5 μm is prevented by the size of nano-emulsions below 200–300 nm. Then, their elimination is performed by the macrophages of the reticuloendothelial system (RES) and particularly in liver and spleen. Küpfer cells in liver are particular macrophages very efficient for nanoparticles uptake; they are located in the border of hepatic sinuses, and constitute 25 % of the

liver cells and 90 % of the macrophages in the body. Spleen is well an efficient trap for nanoparticles. Then, their elimination is performed through the bile by transcytosis within the gall bladder. On the other hand, when the particles are smaller than 5–10 nm they are filtrated by kidneys, and this happens in some applications with, *e.g.* micelles or small hydrophilic contrast agents.

It appears that the therapeutic efficiency of drugs can be improved by their potential targeting through nano-carriers, and thus depend on their time of circulation in the blood stream. The longer is this circulation time, the longer will be the contact with the target tissues. It follows that increasing the circulation time of the nanocarriers in bloodstream (*i.e.* making them stealth towards RES) is a key factor for improving the drug efficiency. Actually, before the macrophage uptake by phagocytosis as discussed above, the nanoparticles are recognized through opsonization, by fixation onto their surface of blood proteins called opsonin. Two parameters are known to inhibit this phenomenon, the size of the particles and the chemical nature of the surface. Indeed, the limit of 100 nm is generally considered as an efficient limitation of the RES recognition, as well as the decoration of the surface with neutral hydrophilic polymers like polyethylene glycol (PEG).

In the case of nano-emulsions, we have seen that the different formulation processes give rise to oil nano-droplet suspensions of similar physicochemical properties. Therefore the size and surface composition should be mainly related to the choice of stabilizing agent. Precisely, a large class of stabilizing agents, *i.e.* nonionic surfactants, fulfills such specifications and allows the simple formulation of small PEGylated nano-droplets. Nonionic surfactants are generally composed of a PEG chain as hydrophilic part connected to a more or less simple aliphatic chain. Owing to their high surfactant properties (HLB > 15–16) they allow to reach very small size below 200 or even 100 nm, and owing to the PEG part of the surfactant the resulting droplets are naturally protected from opsonization. Spontaneous emulsification has emerged as a very efficient method to produce stealth nano-emulsion droplets. Some examples are reported in Fig. 11.4, for different kinds of nanoparticles comparing nano-emulsions, polymeric nanocapsules and inorganic nanoparticles. Their morphologies are illustrated in TEM micrographs and the longitudinal quantification of their concentration in blood are reported for all nanoparticles.

In fact, these nanoparticles differ in their mean sizes, with nano-emulsions around 80 nm, and, inorganic nanoparticles or polymeric capsules around 200 nm. However we have to consider that the size distributions of these kinds of suspensions largely overlap, and thus the average size should not be considered as main factors influencing the blood clearance. Another basic factor that impacts on the blood pharmacokinetics, beyond the surface functionalization, is the nature of the particle core itself. In Fig. 11.4a, blood concentration of nano-droplets (*i.e.* proportional to X-ray contrast) are compared for droplets of similar size and made with the same surfactant (PEG-35 ricinoleate) but with different iodinated oils constituting their core. One can see a slight difference in the curve profiles, resulting in half-lives varying from 6 h to 9 h. However, when the surface is drastically modified with a polymeric capsule (Fig. 11.4b), the clearance is much more decreased up to 2.5 h, and finally reaches 1 h with inorganic (tungsten oxide crystals) (Fig. 11.4c).

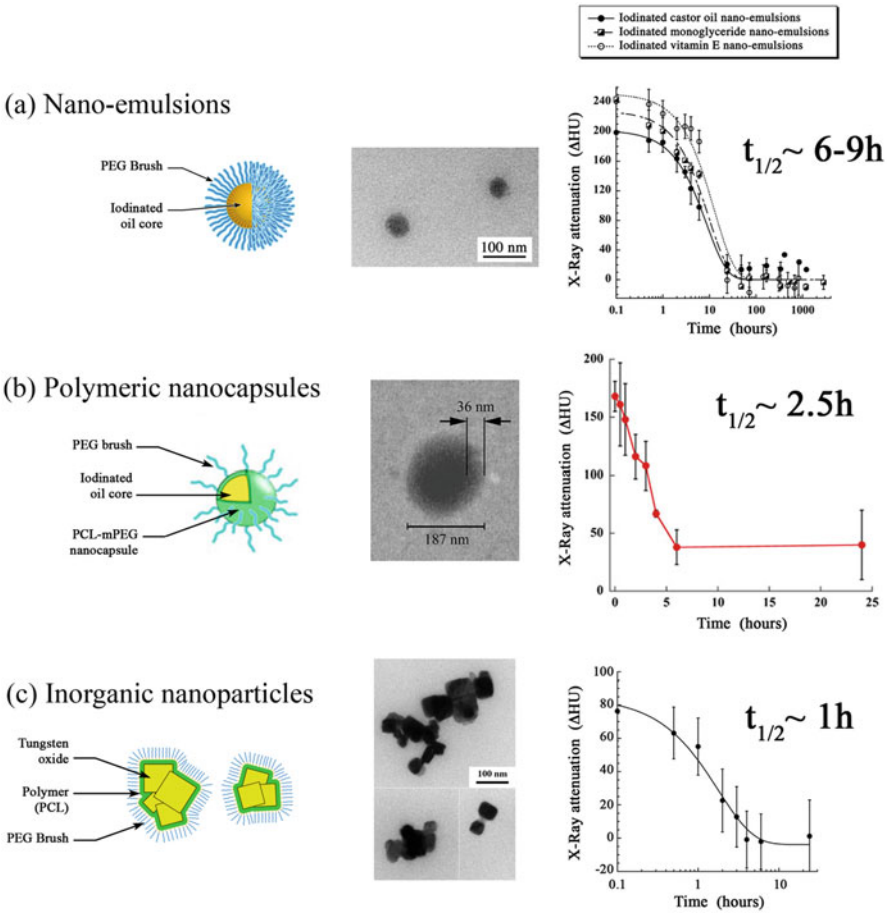

Fig. 11.4 (adapted from (Attia et al. 2014; Hallouard et al. 2013; Jakhmola et al. 2014)) Comparison of the residence time in bloodstream for different kinds of nanoparticles: (**a**) nano-emulsions, (**b**) polymeric nano-capsules, and (**c**) inorganic nanoparticle. The figure presents a schematic illustration of the nanoparticle structure (*left*), transmission electron micrograph (*middle*), and X-ray attenuation (proportional to the blood concentration of nanoparticles) in function of time post-intravenous administration in mice

Obviously the nature of the nanoparticles influence the opsonization process due to the surface charge, electronic density or protein attractions by other low-energy forces (Owens and Peppas 2006), but we can note as well that in the case of nano-emulsions the PEG coverage is actually optimal since any other material enters in the surface composition.

Besides the considerations on blood circulation time, the drug targeting process is associated to the nano-carriers accumulation into the aimed tissues during this blood circulation phase. This means that it is related to accumulation phenomena, specific to the nature of the nano-carrier and/or surface functionalization. This

accumulation can be the direct consequence of the size, chemical nature or charge of the nano-carriers (so-called passive targeting), but can also be induced by the decoration of the surface by ligands specific to the receptors overexpressed in the target tissues (so-called active targeting). Sometimes the natural elimination pathways of the vectors towards the liver or spleen are used for the specific drug delivery in these organs, and can be also called passive targeting (of liver or spleen). In this case, we have disclosed the passive accumulation in these organs thanks to X-ray imaging that allows the longitudinal non-invasive *in vivo* quantification of the biodistribution. Figure 11.5 illustrates the biodistribution in liver, spleen and kidney of nano-emulsions with similar size and physicochemical properties, but different oil cores made with iodinated vitamin E, iodinated castor oil, and iodinated monoglyceride (as in Fig. 11.4a above). The quantification of their biodistribution with time emphasize drastic differences between the different organs, iodinated vitamin E is more accumulated in liver while iodinated castor oil prefers spleen, and on the contrary iodinated monoglyceride does not show an organ specificity and is simply more rapidly eliminated from the organism. It follows that the passive accumulation of nano-droplets through elimination pathway is a powerful tool for imaging pathologies actually located in these organs as described in (Almajdub et al. 2007; Martiniova et al. 2010; Aprahamian et al. 2011; Boll et al. 2011) in liver and spleen.

On the other hand, passive targeting includes the passive accumulation in tumors, for instance implanted subcutaneously, and considered to be undergone through the enhanced permeation and retention effect (EPR effect), targeting. EPR effect results from the passive accumulation of drug or nanocarriers due to their extravasation through leaky vasculature. It is well established that for certain pathologies like tumors, infarctus, inflammation areas, and under certain circumstances, the endothelial lining of the blood vessel wall becomes more permeable than in the normal state (Hobbs et al. 1998; Jain 1999). Thus, large molecules and nanoparticles ranging from 10 to 500 nm can leak from the vessel and accumulate in interstitial space, *i.e.* co-localize with the pathology. Actually, the efficiency of the passive EPR tumor accumulation is basically related to the time of the agent in bloodstream: the higher is the exposure, the higher is the accumulation. Thus, a prolonged time in blood is obtained with non-renal clearable entities (size > 5 nm) (Fang et al. 2001) decorated with well solvated and flexible polymer chain (PEG) was shown to slow down their opsonization and clearance by the RES (Klibanov et al. 1990; Torchilin and Trubetskoy 1995). The major examples reported in literature refer to liposomal formulations that accumulate in subcutaneous xenografted tumors (Karathanasis et al. 2009; Zheng et al. 2009; Anayama et al. 2013). The direct visualization of this accumulation phenomenon is provided by X-ray imaging techniques, and reveals the gradual enhancement of the contrast over time in the tumor surrounding regions. Some examples of EPR targeting with nano-emulsions were reported and have proved the compatibility of lipid droplets with EPR effect in general. For instance, in Ref. (Khalid et al. 2006), the authors report the formulation of nano-emulsions made with PEGylated surfactants (PEG 660-hydroxystearate) stabilizing medium chain triglyceride core. These lipid nano-droplets encapsulated anticancer mole-

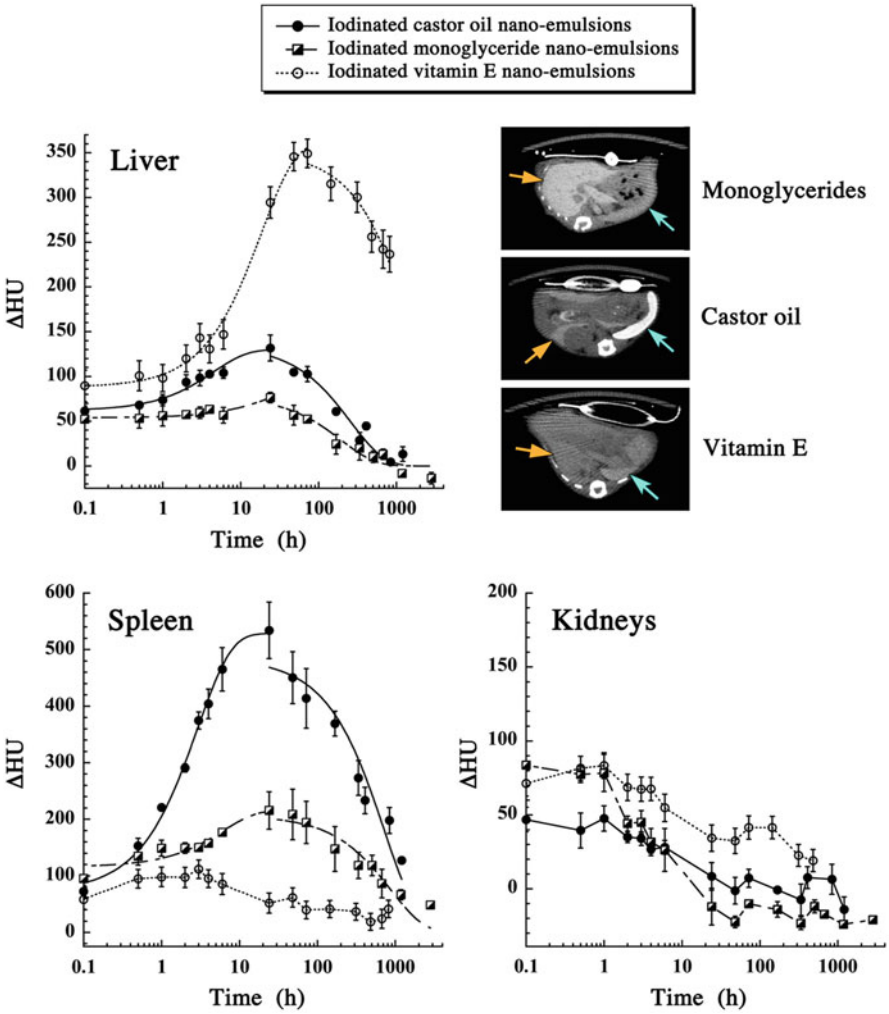

Fig. 11.5 (adapted from Ref. (Attia et al. 2014)) Quantification of the droplet concentration in liver, spleen and kidneys (through X-ray attenuation, ΔHU) after i.v. administration of iodinated nano-emulsions with similar size and physicochemical properties, but different oil cores made with iodinated vitamin E, iodinated castor oil, and iodinated monoglyceride. To illustrate the differences in contrast at 24 h post-injection, transverse slices through the liver and spleen are presented. Liver is indicated by orange arrows and spleen by blue arrows (n = 3 mice/group)

cule, docetaxel (DTX), at a concentration of 3 wt.% of the nano-droplet. The passive EPR accumulation the model tumor occurred thanks to the nano-carriers, studied and compared to a commercial control formulation (*i.e.* solubilized in micelles) of DTX (Taxotere®, TXT). C26 colon adenocarcinoma cells in growth medium were injected subcutaneously in three different locations on the back of each mouse, which produced three separate tumors. The formulations were admin-

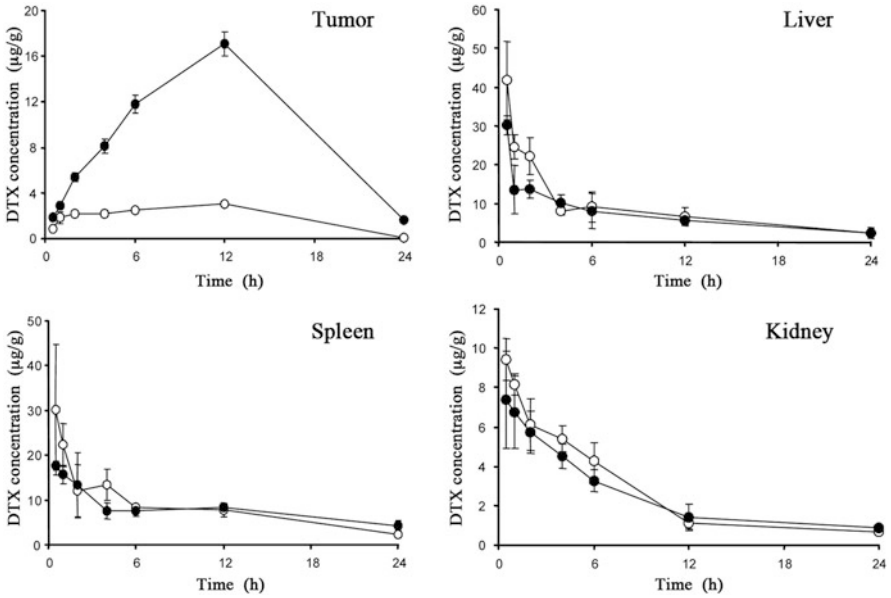

Fig. 11.6 (adapted from Ref. (Khalid et al. 2006)) Illustration of the passive targeting of nano-emulsions to xenografed subcutaneous tumor in mice after i.v. administration of nano-emulsions encapsulating DTX (*closed circles*) and of control injection of TXT (*open circles*). The drug dose level of 15 mg/kg and the concentration in the nanocarrier is 3 wt.% (n = 4 mice/group)

istered when each tumor grew to a volume of about 20 mm^3, approximately 10 days after cell inoculation. These results are reported in Fig. 11.6, where the two above-described formulations were injected at similar doses of 15 mg/kg, comparing the pharmacokinetics and biodistributions of DTX in tumor. The results disclose a clear-cut and significant accumulation in tumor of the DTX encapsulated in nano-emulsions compared to the control roughly constant, while in liver, spleen and kidney the two curve profiles are similar. This clearly evidences the EPR effect induced by the lipid nano-carrier.

Actually in literature, EPR accumulation is generally illustrated with liposomes, for example in biomedical imaging (Karathanasis et al. 2009; Zheng et al. 2009; Anayama et al. 2013; Li et al. 2014). Herein for nano-emulsions, a similar size range and lipid nature gives rise to the similar efficiency in the passive accumulation of lipid nano-emulsion droplets in tumors, that can allow to draw a realistic parallel with the liposomes EPR accumulation. As a last remark, the active targeting of nano-emulsions, performed with post-insertion in nano-emulsion droplets of function lipids, remains anecdotal and not very efficient (Béduneau et al. 2008), likely due to the difficulty to increase the ligand concentration decorating the particle surface.

11.3.2 Clinical Applications of Nano-emulsions

Some nano-emulsions have already clinical applications and are authorized in different countries. We will present you in this part, different applications of such commercialized emulsions. Then, a description of current clinical assays on nano-emulsions will be performed. Mainly, nano-emulsions in commercialized formulations are used to improve drug solubility in water and therefore drug bioavailability. To illustrate these facts one can mention two examples. The first is Neoral® (Novartis Pharma, Rueil-Malmaison, France), an oral cyclosporine emulsion for transplantation (ANSM). The second is Propofol Lipuro® (B Braun AG, Melsungen, Germany), an emulsion of propofol in soy oil for intravenous administration (ANSM). This last is used for anesthesia in intensive care units. Another advantages of nano-emulsions are the possibility to inject oil intravenously and to improve emulsion stability. This is for example the case for Medialipide® (B Braun Medical, Boulogne, France), a commercialized oil-in-water emulsified lipid utilized for parenteral nutrition (ANSM). To be administrated, strictly speaking oil droplets size should be less than 5 microns but in practice the characterizing size is the average size of the lognormal distribution meaning that the population contains droplets much bigger than the average size. It follows that nano-emulsions to be compatible with parenteral administration have a size range below the micrometer.

We identified the current clinical assays on nano-emulsions using the Cochrane library. It is noteworthy that in this part, we will not present the assays using nano-emulsions as model for the evaluation of different treatments or drugs on hyperlipidemia. Experiments based on *ex vivo* model like explanted human tooth are likewise not considered.

Actually, these clinical assays could be classified in 3 applications: anesthesiology, dermatology and vaccines. One publication concerned a comparative study of emulsified propofol with Solutol® HS15 (BASF) in nanometric size and propofol in soybean oil emulsion for anesthesia during endoscopy. This phase II assay was performed on 150 patients (being 33–54 years old) (Rodrigues et al. 2012). The authors observed equivalence between emulsified propofol and propofol in nanometric emulsion form concerning its efficacy, safety and the side effects. However, it is worth to note that it was a lower incidence of pain during injection with propofol in nanometric emulsion form: 53.3 % of patients instead of 82.7 % with propofol in soybean oil emulsions. In additions, the incidence of nausea and vomiting was reduced with nano-emulsified propofol from 10.7 to 2.7 % of the patients. A lack of this work is the absence of comparative study with Propofol Lipuro®, propofol emulsion containing medium-chain triglycerides (Dubey and Kumar 2005). Indeed, this last formulation induced less injection pain than non-lipid forms of propofol. A hypothesis was a reduction or an absence of free propofol with Propofol Lipuro®. With a comparative study between Propofol Lipuro® and nano-emulsified propofol with Solutol® HS15 could be a good approach to verify this hypothesis.

Concerning dermatological applications, different applications of nanometric emulsion based drugs are clinically tested. A first clinical assay was conducted on

482 subjects for the development of drug against cold sores (Kircik et al. 2012). The developed active substance (NB-001) was formulated at different dosages (0.1, 0.3 or 0.5 wt.%) in nanometric emulsions. At the first signs or symptoms of a cold sore episode, this medicine was applied 5 times per day, approximately 3–4 h apart, for 4 days. Emulsions at a drug concentration of 0.3 wt.% showed the best efficiency by a 1.3 days improvement in the mean time to healing compared to placebo ($p = 0.006$). This could be explained by a better skin penetration of the active substance at this concentration. Concerning drug safety, no serious side effects or dermal irritation at any concentration were observed. In additions, no active substance was detected in subject bloods. Compared to other medicine for cold sores, the observed efficacy was similar to oral nucleoside analogues and greater than topical formulations which present a reduction of healing time by only one half day. The originality of this new formulation is the lack of drug distribution in blood preventing most of side effects for an efficacy comparable to oral formulations.

The two next studies focused on drug evaluation for the treatment of distal subungual onychomycosis (Ijzerman et al. 2010a, b). The formulation consisted of emulsions with a mean droplet size of 180 nm containing a new active substance (NB-002). The first study corresponds to a phase II assay on 432 subjects having mild to moderate subungual onychomycosis of the toenails (Ijzerman et al. 2010a, b). The treatment was applied to all toenails and on 5 mm of adjacent skin for 42 weeks. The droplet size and emulsion composition allow selective uptake into the skin without irritation via hair follicles and skin pores. In additions, the droplet size of the formulation destabilized fungal hyphae and spores leading to a formulation efficiency of 84 % compared to 13 % with blank emulsion. No serious side effect was observed during this assay. Nevertheless, the most observed side effect was nail discoloration and concerned globally 10 subjects on 432. The second assay is a post-hoc analysis of the first study on 227 subject to assess the post-treatment mycologic cure and effective treatment rates of a 42-week treatment regimen of NB-002 compared to vehicle (Ijzerman et al. 2010a, b). At 4 and 8 weeks post-treatment, an evaluation of the treatment efficiency. At all emulsion concentration of NB-002, the mycologic cure rates 8 weeks post treatment was ranged from 4.2 to 16.9 % versus 5.3 % in blank emulsion. These assays showed clear antifungal activity with clinically significant nail clearing of NB-002. For more, the emulsion form had also an activity on treatment efficacy.

Several phase III assays concerned the use of nano-emulsions of BF200 5-aminolaevulinic acid (BF200 ALA) for actinic keratosis (AK) photo-treatment compared to a registered 5-aminolaevulinic acid cream (MAL) or placebo (Szeimies et al. 2010; Dirschka et al. 2012; Dirschka et al. 2013; Neittaanmäki-Perttu et al. 2014). BF-200 ALA (Biofrontera Bioscience GmbH) is a gel formulation of 5-aminolaevulinic acid (ALA) with nano-emulsion. This formulation was designed to prevent ALA instability and improve skin penetration (Szeimies et al. 2010; Dirschka et al. 2012). For the illumination, different devices were used 3 h after drug administration: narrow emission spectrum LED (590–670 nm; Aktilite CL128®) or broad emission spectrum LED (580–1400 nm; PhotoDyn 750®). These assays were performed on 13–663 patients presenting a light to mild AK on face

and/or bald scalp. The protocol included one drug application followed by a LED luminescence. In cases of residual AK lesions corresponding mostly to grade II and III AK, a second treatment was performed 12 weeks after the first (Dirschka et al. 2013; Neittaanmäki-Perttu et al. 2014). Then, patients where followed during 3–12 months to determine influence of different treatment protocols on AK recurrence (Szeimies et al. 2010; Dirschka et al. 2013; Neittaanmäki-Perttu et al. 2014). Concerning the results, since 2010 and confirmed by all other works, the authors concluded that treatment efficacy depends on both drug design and luminescence technique. Narrow spectrum light sources presented the best results. For example, on 600 patients with MAL or BF200 ALA, this technique had a healing rate compared to broad spectrum lamps of 71.5 % versus 61.3 % and 84.8 % versus 65.7 % respectively (Dirschka et al. 2013). It was to note that only with placebo broad spectrum lamps had better results 21.6 % versus 12.8 % with narrow spectrum light sources. In point of view of used drug formulations, BF200 ALA presented the best efficacy compared to MAL and placebo in all assays. The healing rates on 600 patients for BF200 ALA compared to MAL were 78.2 % versus 64.2 % ($p = 0.05$) with a remission rate at 3 months for BF200 ALA of 90.4 % (Dirschka et al. 2013). This difference could be explained by the observation on 13 patients of better histological clearance at 3 month with BF200 ALA compared to MAL: 61.5 % compared to 38.5 % ($p = 0.375$) (Neittaanmäki-Perttu et al. 2014). At 12 months after last treatment, BF200 ALA showed the best remission rates at 47 % versus 36 % for MAL (Dirschka et al. 2013). Concerning the safety of BF200 ALA, the observed side effects were similar with MAL (Dirschka et al. 2013; Neittaanmäki-Perttu et al. 2014). All these results demonstrated that BF-200 ALA is a very effective and superior to a registered MAL. In additions efficacies and adverse events are also depended to the different light sources used.

Two publications report vaccines against influenza (Stanberry et al. 2012; Treanor et al. 2013). In both assays, emulsions had the role of adjuvant. In the first work, the authors used a glucopyranosyl lipid A, an emulsion designed to be an intramuscular vaccine (Treanor et al. 2013). They performed a phase I/II assay on 392 patients (being 18–49 years old) receiving two administrations at D1 and D21. Forty two days after the first vaccine administration, up to 82 % of the tested patients presented seropositivity to the different influenza stems. Concerning vaccine security, this study revealed that the half of patients presented light to mild side effects. In some cases, the authors determined serious side effects requiring the use of antihypertensive drugs. In the second work, the author used a new adjuvant W805EC corresponding to nano-emulsion. Indeed, nasal mucosa is the main entry for influenza virus (Stanberry et al. 2012). The authors performed a phase I assay on 199 patients receiving a single intra-nasal administration of vaccine for 3 different influenza strains. The innovation was to design a vaccine for an intra-nasal administration in order to induce both systemic and mucosal immunity. Despite immunization process with a single administration through an original administration route, more than 70 % of the volunteers were sero-protected for the 3 influenza strains through systemic and mucosal immunity. W805EC as adjuvant presented a good tolerance during this clinical assays: absence of serious side effects and observation of side effects similar with intra-nasal administration of PBS (Phosphate buffer saline).

11.3.3 Nano-emulsions in Biomedical Imaging

Another fundamental application of nano-emulsions concerns their use as contrast agents for biomedical imaging. The formulations strategies can be actually close to the formulations of medicines, with on the whole different purposes. Imaging is an important preliminary aspect of some treatments like cancer treatment, providing real-time monitoring with minimal invasiveness and tissue destruction. Biomedical imaging is often used for prediction, screening, staging, prognosis, biopsy guidance, therapy planning, and guidance. Computed X-ray tomography, magnetic resonance imaging, fluorescence and ultrasound have been traditional techniques of anatomical imaging. Ultrasound is commonly used as an external stimulus due to its accessibility, cost-effectiveness, and ability to be used in conjunction with multimodal systems. Besides, optical imaging tools, PET, SPECT, and photoacoustic imaging techniques, nano-emulsions have been widespread used in biomedical fields, daily consuming, particularly in cosmetics and even food industry owing to the huge stability, the encapsulation efficiency, and the high safety of these nano-emulsions.

As mentioned above, the key to their success hinges on their oily cores which act as reservoir allowing solublization and nano-encapsulation of hydrophobic molecules like drugs, contrast agents, organic fluorophores, and/or inorganic NPs at very high concentrations. Other fundamental point for their applications *in vivo* is the non-toxicity since there are lonely fabricated with parenteral-compatible materials. Herein we will shed more light on specific examples to show the importance of the excellent behaviors of nano-emulsions as contrast agent for imaging. And this could be categorized into integrated classes:

11.3.3.1 Nano-emulsions in X-ray Imaging

One of the earliest developed contrast agents-based nano-emulsions for micro-computed tomography (CT) are Fenestra VC® and Fenestra LC® in order to overcome the incompatibility of clinic products like small hydrophilic iodinated molecules. These latter undergo a rapid elimination from the kidneys causing renal failure and do not allow performing scans in preclinical studies.

Introducing the nanotechnology into the medicine made significant progress in micro-CT imaging. Over the last few years, our group has developed several efficient formulations of nano-emulsion-based contrast agents for preclinical X-ray imaging. The ideal solution to ensure a high encapsulation and prevent any release is the synthesis of oily molecules grafted with X-ray contrasting atoms like iodine, and then formulated as nano-emulsions. These droplets are coated with hydrophilic polymer (PEG) to reduce their opsonization that prolongs their residence time in the blood stream. For these applications, as discussed above, the size in the range is 50–250 nm, avoiding a fast clearance by the reticulo-endothelial system (Kulkarni and Feng 2013), but as well large enough to prevent a rapid elimination by kidneys (Choi et al. 2007). From these considerations, some examples of iodinated nano-

emulsions were proposed as contrast agents for X-ray micro CT such as iodinated α-tocopherol nano-emulsions (Li et al. 2013), iodinated monoglyceride nano-emulsions (glyceryl monocaprylate), iodinated triglyceride nano-emulsions (castor oil) (Attia et al. 2014), and iodinated cholecalciferol nano-emulsions (Attia et al. 2015) and studied *in vivo*. The preclinical investigations, briefly discussed in the previous sections, concerned the pharmacokinetics, biodistributions, toxicity and contrasting efficiencies of nano-emulsions, eventually disclosing their outstanding efficacy for X-ray biomedical imaging.

11.3.3.2 Nano-emulsions in Magnetic Resonance Imaging (MRI)

It is approved that some moieties like iron oxide nanoparticles (IONPs), Gd^{3+} chelates, and/or perfluorocarbons PFCs in combination with MRI modality are able to enhance the imaging performance. We will restrain here on the nano-emulsion formulations loading those contrast agents, and it is as well to note that many other examples reports association of MRI contrast agent combined with imaging agents for other modalities.

Recently, a multifunctional and biodegradable nanocarrier system based on oil-in-water nano-emulsions with three different mean diameters (30, 60, and 95 nm) were developed, and used as tumor targeting agent through EPR effect (Jarzyna et al. 2009). The formulation is performed with iron oxide nanoparticles having a hydrophobic coating, dispersed in the soybean oil, solubilizing simultaneously a near infrared fluorophore. These nano-emulsions are injected in nude mice and their accumulation in subcutaneous tumors followed. The optimized quantity of iron oxide nanocrystals induces a remarkably high transverse relaxivity (R2), which is desirable for T2-weighted MRI imaging. The multimodal *in vivo* MRI and fluorescence imaging is shown in Fig. 11.7.

Another example of MRI imaging with nano-emulsions concerns the use of perfluorocarbons (PFCs) as oily phase. PFCs are synthetic organic compounds in which all or most of the hydrogen atoms have been replaced with fluorine atoms. The ^{19}F isotope of PFC's is biologically and chemically inert and thus provides excellent sensitivity *in vivo*. PFCs nano-emulsions have been used for ^{19}F MRI cell tracking (Nöth et al. 1997; Ahrens et al. 2005; Lanza et al. 2005; Partlow et al. 2007) as an alternative to superparamagnetic iron oxide (SPIO) agents, thanks to the high Nuclear magnetic resonance (NMR) sensitivity of the ^{19}F atom. As well, they have been shown to label *in vivo* the monocytes and macrophages, and give positive signals at sites of inflammation (Nöth et al. 1997; Flögel et al. 2008).

11.3.3.3 NEs as Fluorescent Probes in Fluorescent Imaging

Fluorescence is one of the most powerful and commonly used tools in biophysical studies of biomembrane structure and dynamics that can be applied on different levels, from lipid monolayers and bilayers to living cells, tissues, and whole

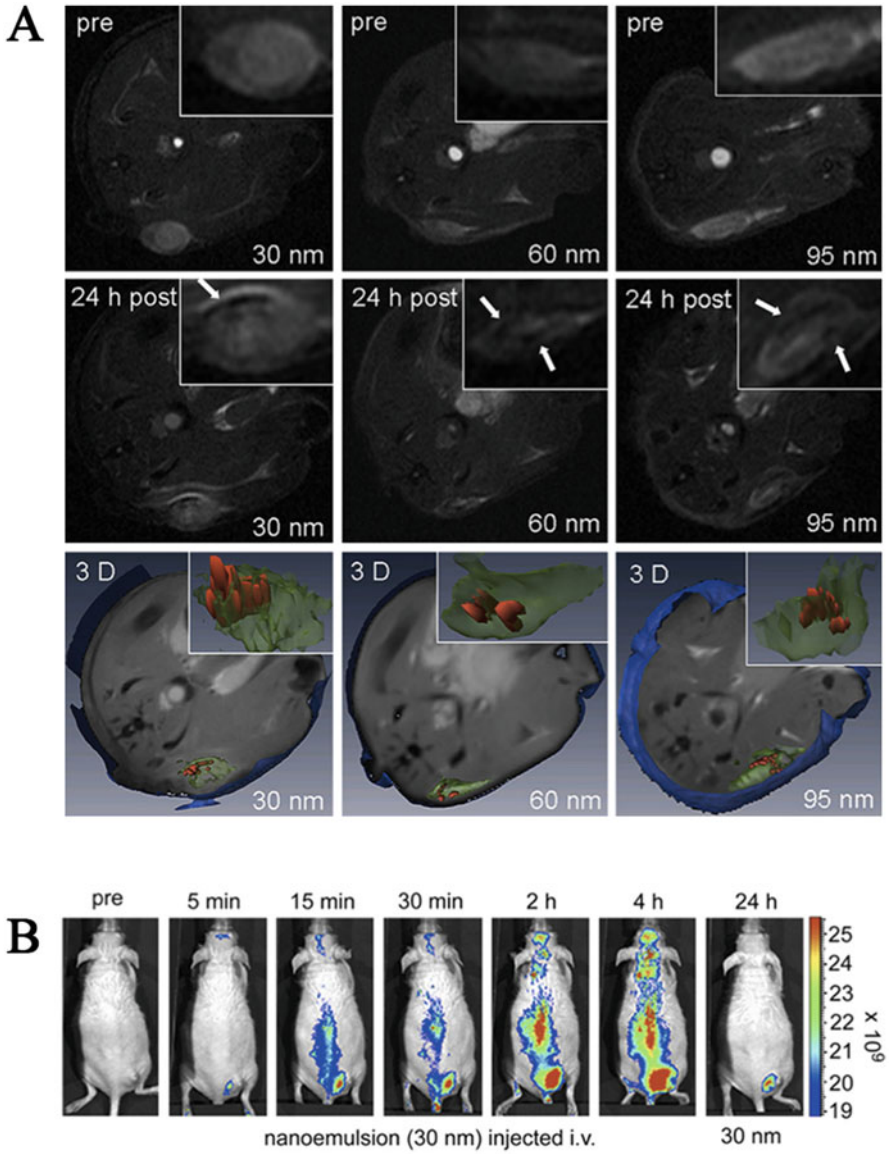

Fig. 11.7 (adapted from (Jarzyna et al. 2009)) MRI images of nude mice bearing subcutaneous EW7 tumors, injected with the three different nano-emulsions of 30 nm, 60 nm and 90 nm. (**a**) T2-weighted MRI images of the pre-scans,, after 24 h after intravenous injection, and 3D images that show the proton density MR image (*grey*), the whole tumor in 3D (*transparent green*) and the areas of iron oxide deposition in red. (**b**) *In vivo* near infrared (*NIR*) fluorescence imaging series showing the accumulation of the 30 nm nano-emulsion

animals. Nano-emulsions are also very suited for encapsulating fluorescent probes at high concentrations either organic dyes or inorganic quantum-dots (QDs), thus enabling a multimodal imaging as shown previously in Fig. 11.7. We have shown that the slight modification of classical dyes enable the increase of their concentration in oil without an excessive loss of quantum yield, resulting in ultrabright nano-droplets with no dye leakage (Klymchenko et al. 2012). This can be performed using classical dyes derivatives, like Nile Red. Actually, we disclosed that in living animal model (zebrafish), classical Nile Red dye encapsulated in nano-emulsions shows a strong release towards the surrounding tissues, whereas modified lipophilic Nile Red does not leak and allows accurate imaging of the blood. In 2010, Goutayer et al. (2010) were able to formulate a lipid nanoparticles (LNP) loading lipophilic fluorescent dye (DiD), then functionalized with the cRGD peptide binding to $\alpha v\beta_3$ integrin, a well-known angiogenesis biomarker, allowing their *in vivo* tracking using fluorescence imaging. *In vitro* study on HEK293(β3) cells over-expressing the $\alpha v\beta_3$ integrins demonstrates the functionalization, specific targeting, and internalization of cRGD-functionalized LNP in comparison with LNP-cRAD or LNP-OH used as negative controls. Following their intravenous injection in Nude mice, LNP-cRGD can accumulate actively in slow-growing HEK293(β3) cancer xenografts, leading to tumor over skin fluorescence ratio of 1.53 ± 0.07 (n = 3) 24 h after injection. Figure 11.8 indicates the *in vivo* imaging in the study.

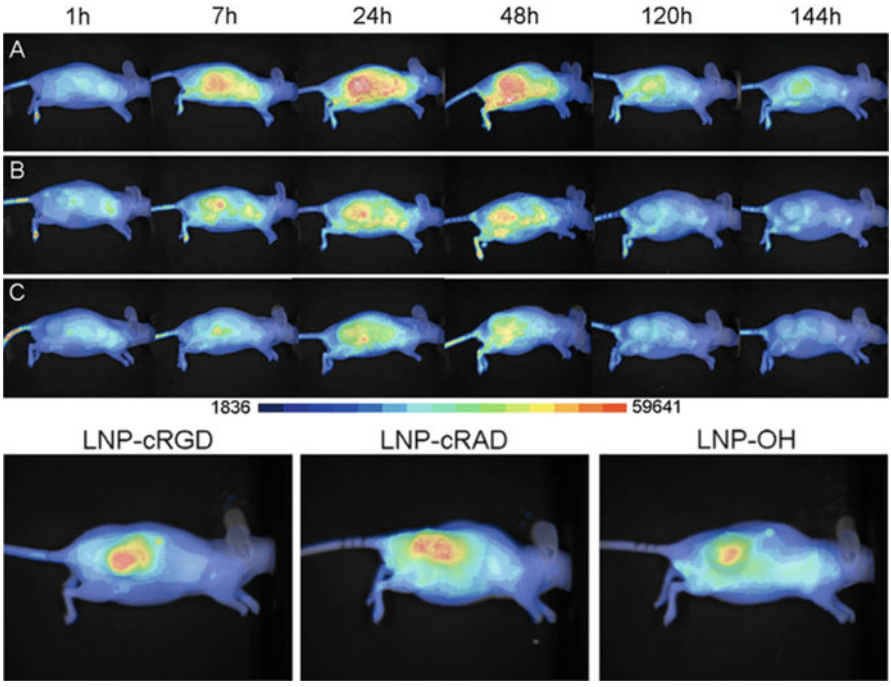

Fig. 11.8 (adapted from (Goutayer et al. 2010)) *In vivo* injection of LNP-cRGD (**a**), LNP-cRAD (**b**), or LNP-OH (**c**) in HEK293(β3) xenografted nude mice

11.3.3.4 Nano-emulsions as Multimodal Imaging Probes and Theragnostics

The main characteristic of nano-emulsions is their cargo structure that allows solubilizing and dispersing lipophilic compounds in the droplet's core, even if the molecules are very different. This property allows encapsulating different contrast agents for different imaging modalities, but also contrasts agents and drugs, so-called theragnostics agents.

A study has been performed by Jiali Ding et al. (2013) to design CT/fluorescence dual-modal nano-emulsion platform for investigating atherosclerotic plaques. Hydrophobic QDs were embedded in iodinated oil, which subsequently were dispersed in water to form multimodal contrast agent. The simultaneous X-ray contrasting properties and fluorescence properties were proved. These authors show that the nano-emulsion droplets entered murine macrophage cells and human liver cells, conferring them bimodal imaging properties. *In vivo* evaluation on atherosclerotic rabbits showed that bimodal nano-emulsions are detected to target specifically macrophages and allows visualizing atherosclerotic plaques.

On the other hand, the co-encapsulation of contrast agent and drug, *i.e.* theragnostics, has seen a real emergence in the last decade since it opens a real chance to monitor the actual dosage and amount of drug delivery in real time. This is even more interesting when non-invasive imaging techniques are more and more efficient, thus offering the possibility to follow quantitatively the drug targeting within a living organism. An interesting example reports a multimodal theragnostics nano-emulsion, containing MRI and fluorescent contrast agent (IONPs and Cy7, respectively), along with a glucocorticoid prednisolone acetate valerate (PAV) used for cancer treatment (Gianella et al. 2011). The droplets were functionalized with $\alpha v\beta_3$-specific RGD peptides, and administrated in subcutaneous tumors-bearing mice (at doses of 30 mg of FeO/kg and 10 mg of PAV/kg). The results, reported in Fig. 11.9 show a significant accumulation of the contrast agents in the tumor region, while tumor growth profiles revealed a potent inhibitory effect in all of the PAV containing nano-emulsion (compared to the control without PAV).

Another study (Tiwari et al. 2006) was reported for fabrication of DTPA-PE-Gd^{3+} (diethylenetriaminepentaacetic acid phosphoethanolamine) complexes nano-emulsions encapsulating paclitaxel hydrophobic drug and their T1 relaxation times measured. Based on NMR and MRI results, it was concluded that this system could act as a contrast agent. *In vitro* cell experiments also confirmed the drug delivery efficacy of the nano-emulsions, since they penetrated the cell membrane and killed the cancerous cells. O'Hanlon *et al.* (O'Hanlon et al. 2012) have synthesized the NIR-labeled perfluoropolyether (PFPE) nano-emulsions for drug delivery and imaging. In brief, PFPE-tyramide was successfully formulated into a non-steroidal anti-inflammatory drug, celecoxib (0.2 mg/mL)-carrying nano-emulsions with dual imaging modalities, ^{19}F MR and NIR. The results obtained by Dynamic light scattering (DLS), ^{19}F NMR, NIR fluorescence microscopy, and biological studies indicate that the nano-emulsion formulation may be useful for parenteral administration of celecoxib.

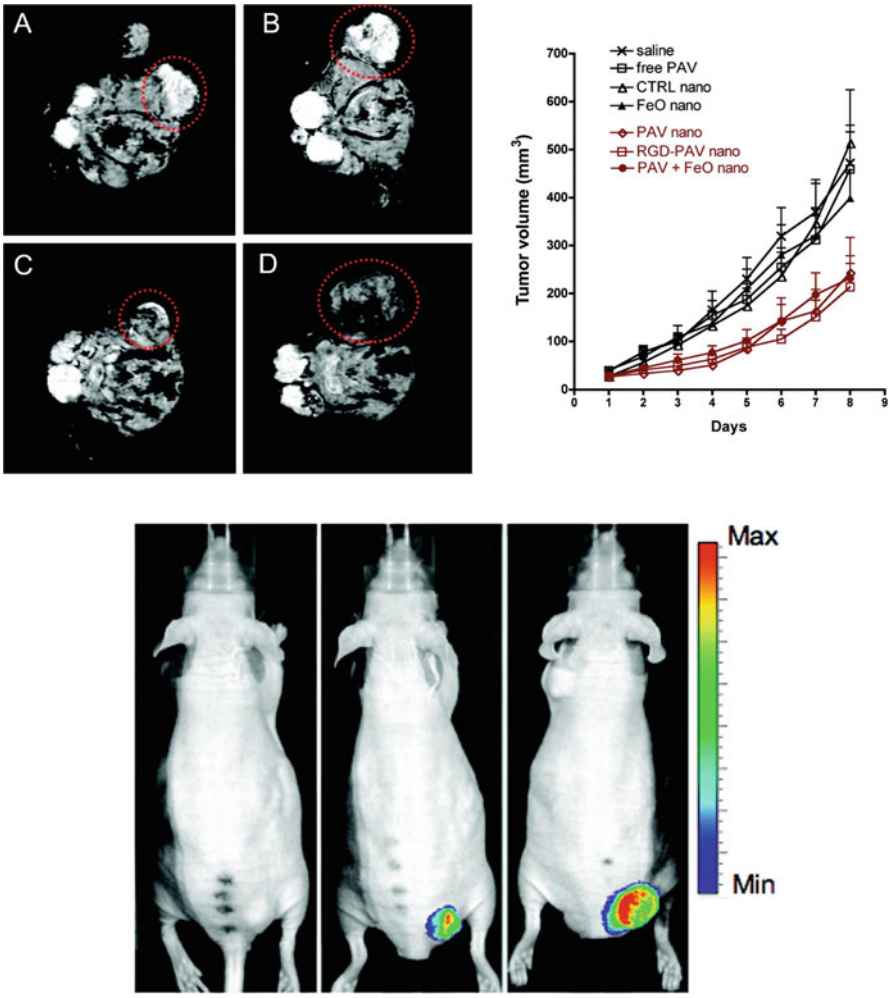

Fig. 11.9 (**a**-**d**) *In vivo* MRI imaging of xenografted tumor in mice (transverse sections), *red circles* indicate the tumors; (**a**) Selected MR images of PAV nano-emulsions and (**b**) control nano-emulsions. (**c**) MR images of PAV + FeO nano-emulsion and (**d**) FeO NE injected mice. *Red circles* indicate the tumors. In (**a**) and (**b**) tumors appeared bright compared to surrounding muscle tissue, and in (**c**) and (**d**), tumor areas appeared hypo-intense, indicative of FeO accumulation. Starting at day 6, tumor growth profiles showed statistically significant tumor growth inhibition ($P < 0.001$) in all of the PAV nano-emulsions treated groups compared to saline, control nano-emulsions, FeO nano-emulsions, and free PAV injected groups. *Bottom: In vivo* NIRF images of a mouse injected with unlabeled NE (*left*) and mice (two different sized tumors) injected with Cy7 NE (*middle* and *right*) at the end of the study. (adapted from.(Ding et al. 2013))

11.4 Conclusion

To summarize, we can say that nano-emulsions are stable nano-cargo with important loading capability. These unique features open the doors of mixing the nature of encapsulating materials, enable a wide range of applications from biomedical imaging to therapies. In addition, any application of nanoparticulate systems is conditioned by the toxicity, biodistribution, pharmacokinetics and potentialities to target specific sites, and this chapter has been precisely focused on these different points to show the extent in which nano-emulsions are promising in many fields related to nanomedicines and imaging.

References

Ahrens ET, Flores R, Xu H, Morel PA (2005) In vivo imaging platform for tracking immunotherapeutic cells. Nat Biotechnol 23(8):983–987

Almajdub M, Nejjari M, Poncet G, Magnier L, Chereul E, Roche C, Manier M (2007) In vivo high-resolution X-ray microtomographyfor liver and spleen tumor assessment in mice. Contrast Media Mol Imaging 2:88–93

Anayama T, Nakajima T, Dunne M, Zheng J, Allen C, Driscoll B, Vines D, Keshavjee S, Jaffray D, Yasufuku K (2013) A novel minimally invasive technique to create a rabbit VX2 lung tumor model for nano-sized image contrast and interventional studies. PLoS One 8, e67355

ANSM. Résumé des caractéristiques du produit – MEDIALIPIDE 20 POUR CENT, émulsion pour perfusion - Base de données publique des médicaments.

ANSM. Résumé des caractéristiques du produit – NEORAL 100 mg/ml, solution buvable - Base de données publique des médicaments.

ANSM. Résumé des caractéristiques du produit – PROPOFOL LIPURO 1 % (10 mg/ml), émulsion injectable ou pour perfusion – Base de données publique des médicaments.

Anton N, Vandamme TF (2009) The universality of low-energy nano-emulsification. Int J Pharm 377:142–147

Aprahamian M, Bour G, Akladios CY, Fylaktakidou K, Greferath R, Soler L, Marescaux J, Egly JM, Lehn JM, Nicolau C (2011) Myo-InositolTrisPyroPhosphate treatment leads to HIF-1α suppression and eradication of early hepatoma tumors in rats. ChemBioChem 12(5):777–783

Attia M, Anton N, Chiper MC, Akasov R, Anton H, Messaddeq N, Fournel S, Klymchenko A, Mély Y, Vandamme TF (2014) Biodistribution of X-ray iodinated contrast agent in nano-emulsions is controlled by the chemical nature of the oily core. ACS Nano 8(10):10537–10550

Attia MF, Anton N, Akasov R, Chiper M, Markvicheva E, Vandamme TF (2015) Biodistribution and toxicity of X-ray iodinated contrast agent in nano-emulsions in function of their size. Pharm Res 33(3):603–614

Béduneau A, Hindré F, Clavreul A, Leroux JC, Saulnier P, Benoit JP (2008) Brain targeting using novel lipid nanovectors. J Control Release 126(1):44–49

Boll H, Nittka S, Doyon F, Neumaier M, Marx A, Kramer M, Groden C, Brockmann MA (2011) Micro-CT based experimental liver imaging using a nanoparticulate contrast agent: a longitudinal study in mice. PLoS One 6:e25692–e25697

Choi HS, Liu W, Misra P, Tanaka E, Zimmer JP, Ipe BI, Bawendi MG, Frangioni JV (2007) Renal clearance of nanoparticles. Nat Biotechnol 25:1165–1170

Delmas T, Piraux H, Couffin AC, Texier I, Vinet F, Poulin P, Cates ME, Bibette J (2011) How to prepare and stabilize very small nanoemulsions. Langmuir 27:1683–1692

Ding J, Wang Y, Ma M, Zhang Y, Lu S, Jiang Y, Qi C, Luo S, Dong G, Wen S, An Y, Gu N (2013) CT/fluorescence dual-modal nanoemulsion platform for investigating atherosclerotic plaques. Biomaterials 34:209–216

Dirschka T, Radny P, Dominicus R, Mensing H, Brüning H, Jenne L, Karl L, Sebastian M, Oster-Schmidt C, Klövekorn W, Reinhold U, Tanner M, Gröne D, Deichmann M, Simon M, Hübinger F, Hofbauer G, Krähn-Senftleben G, Borrosch F, Reich K, Berking C, Wolf P, Lehmann P, Moers-Carpi M, Hönigsmann H, Wernicke-Panten K, Helwig C, Foguet M, Schmitz B, Lübbert H, Szeimies R-M, Group A-CS (2012) Photodynamic therapy with BF-200 ALA for the treatment of actinic keratosis: results of a multicentre, randomized, observer-blind phase III study in comparison with a registered methyl-5-aminolaevulinate cream and placebo. Br J Dermatol 166:137–146

Dirschka T, Radny P, Dominicus R, Mensing H, Brüning H, Jenne L, Karl L, Sebastian M, Oster-Schmidt C, Klövekorn W, Reinhold U, Tanner M, Gröne D, Deichmann M, Simon M, Hübinger F, Hofbauer G, Krähn-Senftleben G, Borrosch F, Reich K, Berking C, Wolf P, Lehmann P, Moers-Carpi M, Hönigsmann H, Wernicke-Panten K, Hahn S, Pabst G, Voss D, Foguet M, Schmitz B, Lübbert H, Szeimies R-M, Group A-CS, Group A-CS (2013) Long-term (6 and 12 months) follow-up of two prospective, randomized, controlled phase III trials of photodynamic therapy with BF-200 ALA and methyl aminolaevulinate for the treatment of actinic keratosis. Br J Dermatol 168:825–836

Dubey PK, Kumar A (2005) Pain on injection of lipid-free propofol and propofol emulsion containing medium-chain triglyceride: a comparative study. Anesth Analg 101(4):1060–1062

Fang J, Nakamura H, Maeda H (2001) The EPR effect: unique features of tumor blood vessels for drug delivery, factors involved, and limitations and augmentation of the effect. Adv Drug Deliv Rev 63:136–151

Flögel U, Ding Z, Hardung H, Jander S, Reichmann G, Jacoby C, Schubert R, Schrader J (2008) In vivo monitoring of inflammation after cardiac and cerebral ischemia by fluorine magnetic resonance imaging. Circulation 118(2):140–148

Gianella A, Jarzyna PA, Mani V, Ramachandran S, Calcagno C, Tang J, Kann B, Dijk WJR, Thijssen VL, Griffioen AW, Storm G, Fayad ZA, Mulder WJM (2011) Multifunctional nanoemulsion platform for imaging guided therapy evaluated in experimental cancer. ACS Nano 5(6):4422–4433

Goutayer M, Dufort S, Josserand V, Royère A, Heinrich E, Vinet F, Bibette J, Coll JL, Texier I (2010) Tumor targeting of functionalized lipid nanoparticles: assessment by in vivo fluorescence imaging. Eur J Pharm Biopharm 75:137–147

Hallouard F, Briançon S, Anton N, Li X, Vandamme TF, Fessi H (2013) Poly(ethylene glycol)-poly(ε-caprolactone) iodinated nanocapsules as contrast agents for X-ray imaging. Pharm Res 30:2023–2035

Hobbs SK, Monsky WL, Yuan F, Roberts WG, Griffith L, Torchilin VP, Jain RK (1998) Regulation of transport pathways in tumor vessels: role of tumor type and microenvironment. Proc Natl Acad Sci U S A 95:4607–4612

Ijzerman M, Backer J, Flack M, Robinson P (2010a) Efficacy of topical nanoemulsion (NB-002) for the treatment of distal subungual onychomycosis: a randomized, double-blind, vehicle-controlled trial. J Am Acad Dermatol 62:AB76

Ijzerman M, Backer J, Flack M, Robinson P (2010b) Forty-two–week safety study of topical nanoemulsion (NB-002) for the treatment of mild to moderate distal subungual onychomycosis: a randomized, double-blind, vehicle-controlled trial. J Am Acad Dermatol 62:AB77

Jain RK (1999) Transport of molecules, particles, and cells in solid tumors. Annu Rev Biomed Eng 1:241–263

Jakhmola A, Anton N, Anton H, Messaddeq N, Hallouard F, Klymchenko A, Mely Y, Vandamme TF (2014) Poly-ε-caprolactone tungsten oxide nanoparticles as a contrast agent for X-ray computed tomography. Biomaterials 35(9):2981–2986

Jarzyna PA, Skajaa T, Gianella A, Cormode DP, Samber DD, Dickson SD, Chen W, Griffioen AW, Fayad ZA, Mulder WJM (2009) Iron oxide core oil-in-water emulsions as a multifunctional nanoparticle platform for tumor targeting and imaging. Biomaterials 30:6947–6954

Karathanasis E, Suryanarayanan S, Balusu SR, McNeeley K, Sechopoulos I, Karellas A, Annapragada AV, Bellamkonda RV (2009) Imaging nanoprobe for prediction of outcome of nanoparticle chemotherapy by using mammography. Radiology 250(2009):398–406

Khalid MN, Simard P, Hoarau D, Dragomir A, Leroux JC (2006) Long circulating poly(ethylene glycol)-decorated lipid nanocapsules deliver docetaxel to solid tumors. Pharm Res 23(4):752–758

Kircik L, Jones TM, Jarratt M, Flack MR, Ijzerman M, Ciotti S, Sutcliffe J, Boivin G, Stanberry LR, Baker JR, N.-S. Group (2012) Treatment with a novel topical nanoemulsion (NB-001) speeds time to healing of recurrent cold sores. J Drugs Dermatol 11:970–977

Klibanov AL, Maruyama K, Torchilin VP, Huang L (1990) Amphipathic polyethyleneglycols effectively prolong the circulation time of liposomes. FEBS Lett 268(1):235–237

Klymchenko AS, Roger E, Anton N, Anton H, Shulov I, Vermot J, Mély Y, Vandamme TF (2012) Highly lipophilic fluorescent dyes in nano-emulsions: towards bright non-leaking nano-droplets. RSC Adv 2:11876–11886

Kulkarni SA, Feng SS (2013) Effects of particle size and surface modification on cellular uptake and biodistribution of polymeric nanoparticles for drug delivery. Pharm Res 30:2512–2522

Lanza GM, Winter PM, Neubauer AM, Caruthers SD, Hockett FD, Wickline SA (2005) 1H/19 F magnetic resonance molecular imaging with perfluorocarbon nanoparticles. Curr Top Dev Biol 70:57–76

Li X, Anton N, Zubera G, Zhao M, Messaddeq N, Hallouard F, Fessie H, Vandamme TF (2013) Iodinated α-tocopherol nano-emulsions as non-toxic contrast agents for preclinical X-ray imaging. Biomaterials 34:481–491

Li X, Anton N, Zuber G, Vandamme TF (2014) Contrast agents for preclinical targeted X-ray imaging. Adv Drug Deliv Rev 76:116–133

Martiniova L, Schimel D, Lai EW, Limpuanfthip A, Kvetnansky R, Pacak K (2010) In vivo micro CT imaging for liver lesions in small animal models. Methods 50:20–25

Neittaanmäki-Perttu N, Karppinen T t, Grönroos M, Tani T t, Snellman E (2014) Daylight photodynamic therapy for actinic keratoses: a randomized double-blinded nonsponsored prospective study comparing 5-aminolaevulinic acid nanoemulsion (BF-200) with methyl-5-aminolaevulinate. Br J Dermatol 171:1172–1180

Nöth U, Morrissey SP, Deichmann R, Jung S, Adolf H, Haase A, Lutz J (1997) Perfluoro-15-crown-5-ether labelled macrophages in adoptive transfer experimental allergic encephalomyelitis. Artif Cells Blood Substit Immobil Biotechnol 25(3):243–254

O'Hanlon CE, Amede KG, O'Hear MR, Janjic JM (2012) NIR-labeled perfluoropolyether nanoemulsions for drug delivery and imaging. J Fluor Chem 137:27–33

Owens DE, Peppas NA (2006) Opsonization, biodistribution and pharmacokinetics of polymeric nanoparticles. Int J Pharm 307:93–102

Partlow KC, Chen J, Brant JA, Neubauer AM, Meyerrose TE, Creer MH, Nolta JA, Caruthers SD, Lanza GM, Wickline SA (2007) 19F magnetic resonance imaging for stem/progenitor cell tracking with multiple unique perfluorocarbon nanobeacons. FASEB J 21(8):1647–1654

Rodrigues TA, Alexandrino RA, Kanczuk ME, Gozzani JL, Mathias LA, Da ST (2012) A comparative study of non-lipid nanoemulsion of propofol with solutol and propofol emulsion with lecithin. Rev Bras Anestesiol 62(3):325–334

Stanberry LR, Simon JK, Johnson C, Robinson PL, Morry J, Flack MR, Gracon S, Myc A, Hamouda T, Baker JR Jr (2012) Safety and immunogenicity of a novel nanoemulsion mucosal adjuvant W805EC combined with approved seasonal influenza antigens. Vaccine 30:307–316

Szeimies R-M, Radny P, Sebastian M, Borrosch F, Dirschka T, Krähn-Senftleben G, Reich K, Pabst G, Voss D, Foguet M, Gahlmann R, Lübbert H, Reinhold U (2010) Photodynamic therapy with BF-200 ALA for the treatment of actinic keratosis: results of a prospective, randomized, double-blind, placebo-controlled phase III study. Br J Dermatol 163:386–394

Taisne L, walstra B, Cabane B (1996) Transfer of oil between emulsion droplets. J Colloid Interface Sci 184:378–390

Tiwari S, Tan YM, Amiji M (2006) Preparation and in vitro characterization of multifunctional nanoemulsions for simultaneous MR imaging and targeted drug delivery. J Biomed Nanotechnol 2:1–8

Torchilin V-P, Trubetskoy V-S (1995) Wich polymers can make nanoparticulates drug carriers long circulating? Adv Drug Deliv Rev 16(2–3):141–155

Treanor JJ, Essink B, Hull S, Reed S, Izikson R, Patriarca P, Goldenthal KL, Kohberger R, Dunkle LM (2013) Evaluation of safety and immunogenicity of recombinant influenza hemagglutinin (H5/Indonesia/05/2005) formulated with and without a stable oil-in-water emulsion containing glucopyranosyl-lipid A (SE+GLA) adjuvant. Vaccine 31:5760–5765

Zheng J, Jaffray D, Allen C (2009) Quantitative CT imaging of the spatial and temporal distribution of liposomes in a rabbit tumor model. Mol Pharm 6(2):571–580